Biochimica et Biophysica Acta 855 (1986) 68–78
Elsevier

BBA 72901

Membrane lipids: preferred conformational states and their interplay. The crystal structure of dilauroylphosphatidyl-*N*,*N*-dimethylethanolamine

Irmin Pascher and Staffan Sundell

Department of Structural Chemistry, Faculty of Medicine, University of Göteborg, Box 33031, S-400 30 Göteborg (Sweden)

(Received August 5th, 1985)

Key words: Phosphatidyl-*N*,*N*-dimethylethanolamine; Crystal structure; Molecular packing; Head group interaction

The conformation and molecular packing of 2,3-dilauroyl-*rac*-glycero-1-phospho-*N*,*N*-dimethylethanolamine ($DLPEM_2$) has been determined by single-crystal analysis ($R = 0.079$). The lipid crystallizes in a triclinic space group ($P\bar{1}$) with a unit cell of $a = 5.64$, $b = 8.20$, $c = 39.86$ Å and $\alpha = 94.5$, $\beta = 90.1$, $\gamma = 101.9°$. The two molecules of the unit cell are related by centro-symmetry and pack tail to tail in a bilayer structure. The zwitterionic head groups are extended perpendicular to the layer plane and interdigitate with the head group dipoles of the adjacent bilayer. The packing cross-section per molecule is 45.2 $Å^2$. The hydrocarbon chains pack with an orthorhombic (O ⊥) subcell and tilt by 33° with respect to the layer normal. The diacylglycerol moiety shows an unusual conformation. The glycerol chain is inclined by 45° with respect to the layer normal and the fatty acid substituted oxygens adopt mutually a $-$*syn-clinal* instead of the more common $+$*syn-clinal* conformation. Head group interactions and molecular conformation of $DLPEM_2$ are compared with the corresponding structural features of phosphatidic acid, phosphatidylethanolamine and phosphatidylcholine. For the diacylglycerol part three minimum energy conformations are observed, which interconvert by rotation and axial displacement of the hydrocarbon chains.

Introduction

N-Methyl- and *N*,*N*-dimethylethanolamine phosphoglycerides occur only in small quantities in mammalian tissue [1], but are more abundant in a number of bacteria [2]. In mammals these lipids are found, particularly in liver, as metabolic intermediates of a stepwise *N*-methylation of PE to PC [1,3]. This methylation process of PE is proposed to be connected to receptor-mediated trans-membrane signaling [4] and coupled with a Ca^{2+} influx into the cell [5].

From a structural-functional point of view the partially methylated ethanolamine lipids represent interesting intermediates of PE and PC. Compared with the latter two abundant and well-characterized membrane lipids, only little is known about the structural properties of the partially methylated derivatives. Recent studies of the thermotropic phase behaviour of *N*-monomethyl and *N*-dimethyl PE [6,7] show that the temperature of the chain melting transition decreases approximately linearly with increasing *N*-methylation. Furthermore, infrared spectroscopic studies [6] indicate a progressive increase in tilt of the hydrocarbon chains which appears to be related to the increasing cross-sectional area of the head groups.

For a proper understanding of the molecular properties detailed structural information on an atomic level is required. The unsubtituted $-NH_3$

Abbreviations: $DLPEM_2$, dilauroylglycerophospho-*N*,*N*-dimethylethanolamine; PE, phosphatidylethanolamine; PC, phosphatidylcholine; *sc*, *syn-clinal* (= *gauche*); *ac*, *anti-clinal* (= *anti-gauche*); *ap*, *anti-periplanar*.

group and the fully methylated -$N(CH_3)_3$ group exhibit fundamental differences with respect to lateral interaction and packing requirement, giving rise to the characteristic differences in the structural behaviour of PE and PC [8,9]. In the present work we report on the conformation, molecular packing and head group interaction of dilauroyl-glycerophospho-*N*,*N*-dimethylethanolamine as revealed by X-ray single-crystal analysis.

Experimental

2,3-Dilauroyl-DL-glycero-1-phospho-*N*,*N*-dimethylethanolamine ($DLPEM_2$) was synthesized by R. Berchtold (Biochemisches Labor, Bern, Switzerland). Minor impurities were removed by recrystallizing the lipid twice from diethyl ether/ethanol solutions. Finally, small needle-like single crystals were grown from a solution (2.5 mg/ml) in diethyl ether/ethanol/water (10 : 1 : 0.05 v/v) at 12°C. In order to increase the size of the crystals they were almost redissolved at 25°C and recrystallized by slow cooling to 12°C. This procedure was repeated several times.

A crystal with the dimensions 0.48 × 0.08 × 0.02 mm was used for data collection with an Enraf-Nonius CAD4F-11 diffractometer. The angular settings of 25 reflections ($9 < \theta < 30°$) were measured to calculate the lattice parameters. Intensity data for one hemisphere of reflection and with $1 < \theta < 65°$ were collected by the $\theta/2\theta$ scan method using monochromatized CuKα radiation. Three intensity-control reflections, which were measured every 2 h, indicated a slight (7%) crystal decay. The intensities were scaled to account for this decay. A total of 6132 independent reflections were recorded and of these 1502 reflections with $I > 3\sigma(I)$ were considered observed. All intensities were corrected for Lorentz and polarization effects but not for absorption or extinction.

Crystal data

Molecular formula $C_{31}H_{62}NO_8P$, space group $P\bar{1}$,

unit cell $a = 5.636(3)$, $b = 8.200(1)$, $c = 39.863(5)$ Å,
$\alpha = 94.56(1)$, $\beta = 90.15(3)$, $\gamma = 101.94(3)°$

$V = 1796$ Å^3, $Z = 2$, $M_r = 607.81$, $D_c = 1.124$ g·cm^{-3},

μ(CuKα) = 10.4 cm^{-1}

The structure was solved by direct methods using the programs MULTAN [10] and DIRDIF [11], which provided the non-hydrogen atom positions. The hydrogen atom positions were obtained from Fourier difference synthesis maps. Refinement was carried out by the full-matrix least-squares method using anisotropic temperature factors for the non-hydrogen atoms. The hydrogen atoms were assigned a common temperature factor ($B = 5$ Å^2). The hydrogen atom parameters were not refined. The refinement was terminated with $R = 0.079$ and $R_w = 0.100$. The weighting scheme used in the later part of the refinement was $w = 1/(1 + ((|F_{obs}| - 26)/28)^2)$ [12]. The form factors used were those given by Cromer and Mann [13]. All calculations have been performed on a DEC system-10 computer using mainly the X-ray 72 program system [14].

Description of the structure

Fractional coordinates and equivalent thermal parameters of the non-hydrogen atoms are given in Table I. Observed and calculated structure factors and anisotropic vibrational parameters can be obtained from this Department. Atom numbering according to the convention by Sundaralingam [9,15] and bond distances and angles are shown in Fig. 1. The two enantiomeric molecules (D and L) in this structure are related by a center of symmetry and have identical bond parameters.

Molecular packing

In Fig. 2 the packing arrangement of $DLPEM_2$ and the extension of the unit cell is shown in views along the *a* and *b* axes. There are two molecules per unit cell arranged tail to tail in a bilayer structure. The molecules of the two opposite bilayer halves are related by centro-symmetry. Thus, as indicated in Fig. 2, L enantiomers and (natural) D enantiomers pack in separate layers on either side of the bilayer center.

The head group dipoles are extended perpendicular to the layer plane and interdigitate with those of the adjacent bilayer. This head group arrangement results in a packing cross-section in the layer plane of $S = 45.2$ Å^2 per molecule. The hydrocarbon chains accommodate to this molecular area by a tilt of 33° with respect to the layer

TABLE I

ATOMIC FRACTIONAL COORDINATES AND EQUIVALENT ISOTROPIC TEMPERATURE FACTORS ($\times 10^2$) FOR NON-HYDROGEN ATOMS OF DLPEM$_2$ ($U_{eq} = 1/3(U_{11} + U_{22} + U_{33})$)

Atom	x	y	z	U_{eq}
P(1)	0.0574 (6)	0.2620 (4)	0.0508 (1)	5.2 (0.2)
N(1)	−0.1951 (16)	0.2802 (11)	−0.0525 (2)	5.0 (0.6)
O(11)	−0.0975 (13)	0.3507 (9)	0.0774 (2)	5.1 (0.5)
O(12)	−0.1423 (12)	0.1621 (8)	0.0237 (2)	4.4 (0.4)
O(13)	0.2152 (13)	0.4066 (9)	0.0360 (2)	5.5 (0.5)
O(14)	0.1685 (14)	0.1356 (9)	0.0654 (2)	6.0 (0.5)
O(21)	−0.1918 (15)	0.4446 (11)	0.1444 (2)	7.0 (0.6)
O(22)	−0.3507 (22)	0.6688 (13)	0.1507 (3)	11.8 (0.9)
O(31)	−0.4893 (18)	0.1428 (12)	0.1592 (2)	9.1 (0.7)
O(32)	−0.6569 (28)	0.2147 (22)	0.2050 (3)	20.9 (1.5)
C(11)	−0.2998 (19)	0.2504 (15)	0.0078 (3)	5.6 (0.7)
C(12)	−0.3537 (19)	0.1842 (14)	−0.0274 (3)	5.0 (0.7)
C(13)	0.0637 (19)	0.2656 (15)	−0.0485 (3)	6.4 (0.8)
C(14)	−0.2835 (26)	0.2312 (16)	−0.0873 (3)	7.3 (0.9)
C(1)	−0.2709 (21)	0.2433 (14)	0.0971 (3)	5.3 (0.7)
C(2)	−0.3868 (21)	0.3542 (15)	0.1207 (3)	5.5 (0.7)
C(3)	−0.5861 (23)	0.2607 (19)	0.1409 (3)	7.6 (1.0)
C(21)	−0.1934 (27)	0.5971 (18)	0.1572 (3)	7.6 (1.0)
C(22)	0.0044 (24)	0.6580 (16)	0.1833 (3)	6.8 (0.9)
C(23)	−0.0088 (23)	0.5447 (18)	0.2120 (3)	7.1 (0.9)
C(24)	0.1998 (23)	0.5989 (17)	0.2374 (3)	6.4 (0.8)
C(25)	0.1886 (24)	0.4859 (17)	0.2656 (3)	6.9 (0.9)
C(26)	0.3977 (23)	0.5301 (18)	0.2901 (3)	7.0 (0.9)
C(27)	0.3898 (24)	0.4152 (18)	0.3184 (3)	7.2 (0.9)
C(28)	0.5983 (24)	0.4619 (19)	0.3437 (3)	7.7 (1.0)
C(29)	0.5801 (25)	0.3467 (17)	0.3718 (3)	7.3 (0.9)
C(210)	0.7864 (27)	0.3898 (20)	0.3968 (4)	8.9 (1.1)
C(211)	0.7692 (29)	0.2794 (22)	0.4255 (4)	10.1 (1.3)
C(212)	0.9670 (34)	0.3177 (26)	0.4504 (4)	12.3 (1.5)
C(31)	−0.5244 (26)	0.1391 (18)	0.1911 (3)	8.2 (1.0)
C(32)	−0.3725 (23)	0.0411 (17)	0.2076 (3)	6.9 (0.8)
C(33)	−0.3620 (22)	0.0686 (17)	0.2459 (3)	6.8 (0.8)
C(34)	−0.1882 (22)	−0.0211 (17)	0.2619 (3)	6.4 (0.8)
C(35)	−0.1758 (24)	0.0056 (16)	0.2995 (3)	6.8 (0.9)
C(36)	−0.0020 (26)	−0.0878 (19)	0.3159 (4)	8.3 (1.0)
C(37)	0.0155 (25)	−0.0606 (17)	0.3533 (3)	7.5 (0.9)
C(38)	0.1920 (24)	−0.1500 (17)	0.3692 (3)	7.3 (0.9)
C(39)	0.2063 (26)	−0.1235 (19)	0.4077 (3)	8.1 (1.0)
C(310)	0.3868 (28)	−0.2092 (20)	0.4242 (4)	8.9 (1.1)
C(311)	0.3993 (33)	−0.1831 (24)	0.4612 (4)	11.4 (1.4)
C(312)	0.5774 (38)	−0.2621 (29)	0.4770 (4)	14.8 (1.8)

normal. As is obvious from Fig. 2A and B the chains thereby are inclined with respect to both the *ac* and the *bc* planes. Laterally the hydrocarbon chains pack in the orthorhombic perpendicular (O ⊥) chain packing mode [16] with subcell dimensions of

$a_s = 4.99(2)$; $b_s = 7.66(2)$; $c_s = 2.53(1)$ Å

The packing cross-section per chain perpendicular to its long axis is 18.95 Å^2.

Polar interaction

The packing arrangement and interaction of the phospho-*N*,*N*-dimethylethanolamine group is shown in Fig. 3. As can be seen in the view

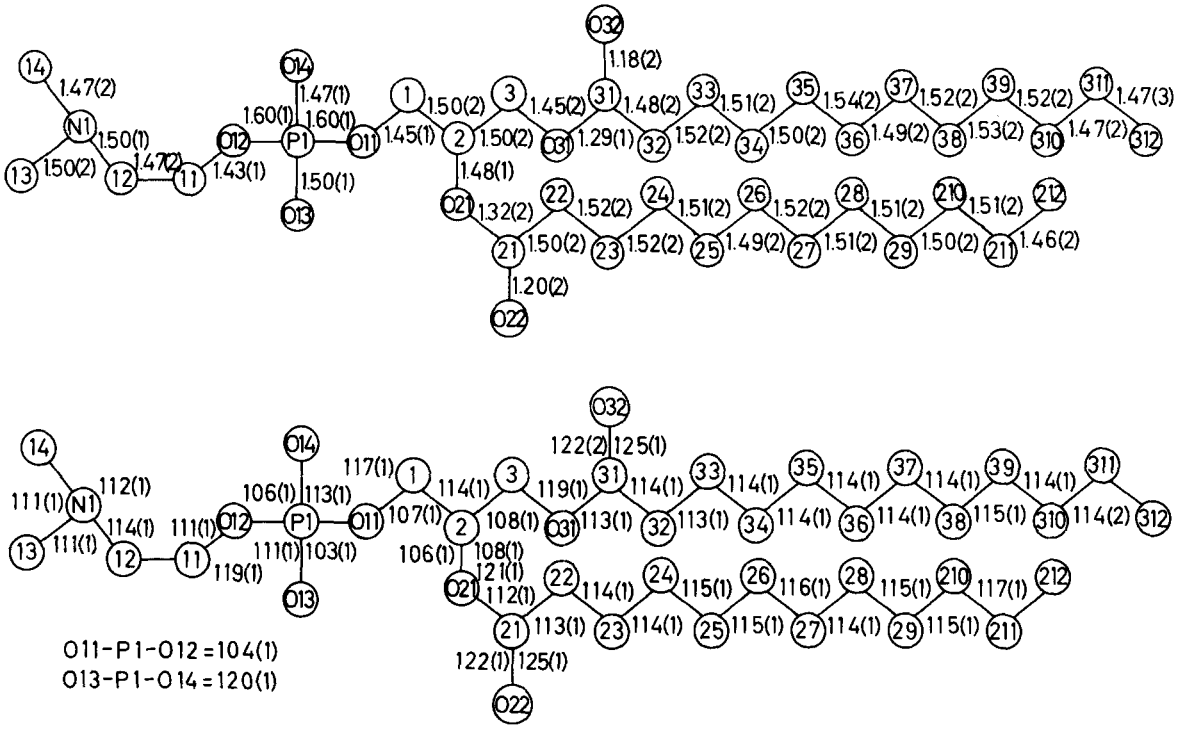

Fig. 1. Atom numbering, bond distances (Å) and bond angles (°) of $DLPEM_2$. The numbering convention according to Sundaralingam [9,15] is used.

parallel to the bilayer interface (Fig. 3A) the head group dipoles are oriented in the direction of the layer normal. The dimethylammonium groups of one bilayer surface extend to the level of the phosphate group of the next bilayer and vice versa. Thus the (+) and (−) charges are equally distributed and located in two, electrostatically neutral planes, 4.0 Å apart.

The ammonium group establishes a short bond (2.63 Å) towards a neighbouring phosphate oxygen (O(13)). This contact is formed in extension of the N–H... bond and has the character of both a hydrogen bond and an ionic contact. Besides the hydrogen bond there are two pure electrostatic contacts (3.4 Å) with the oxygens (O(11) and O(14)) of two adjacent phosphate groups. These interactions are formed towards the nitrogen approximately in the direction of the ...N–C(H) bond axes. A corresponding set of three contacts is formed at the opposite side of the antiparallel P–N dipoles. As is obvious from Fig. 3A and B, all these short intermolecular contacts extend in the *b* direction of the bilayer plane. Surprisingly enough, there are no short intermolecular contacts in the *a* direction.

Molecular conformation

In Fig. 4, the molecular conformation of the natural D enantiomer of $DLPEM_2$ is shown in projections along the unit cell *a* and *b* axes. Torsion angles in comparison to other phospholipids are given in Table II. Note that the L enantiomer has identical torsion angles, but with reverse rotational direction.

The conformation and orientation of the diacylglycerol part of $DLPEM_2$ have rather unusual features: the plane defined by the three glycerol carbon atoms C(1)–C(2)–C(3) is inclined by 45° with respect to the layer plane. From this glycerol carbon plane the two fatty acid substituted glycerol oxygens O(21) and O(31) point 'upwards' towards the bilayer center. This glycerol conformation is produced by a $+sc$ torsion angle ($\theta_3 = 56°$) about the C(1)–C(2)–C(3)–O(31) glycerol bond which

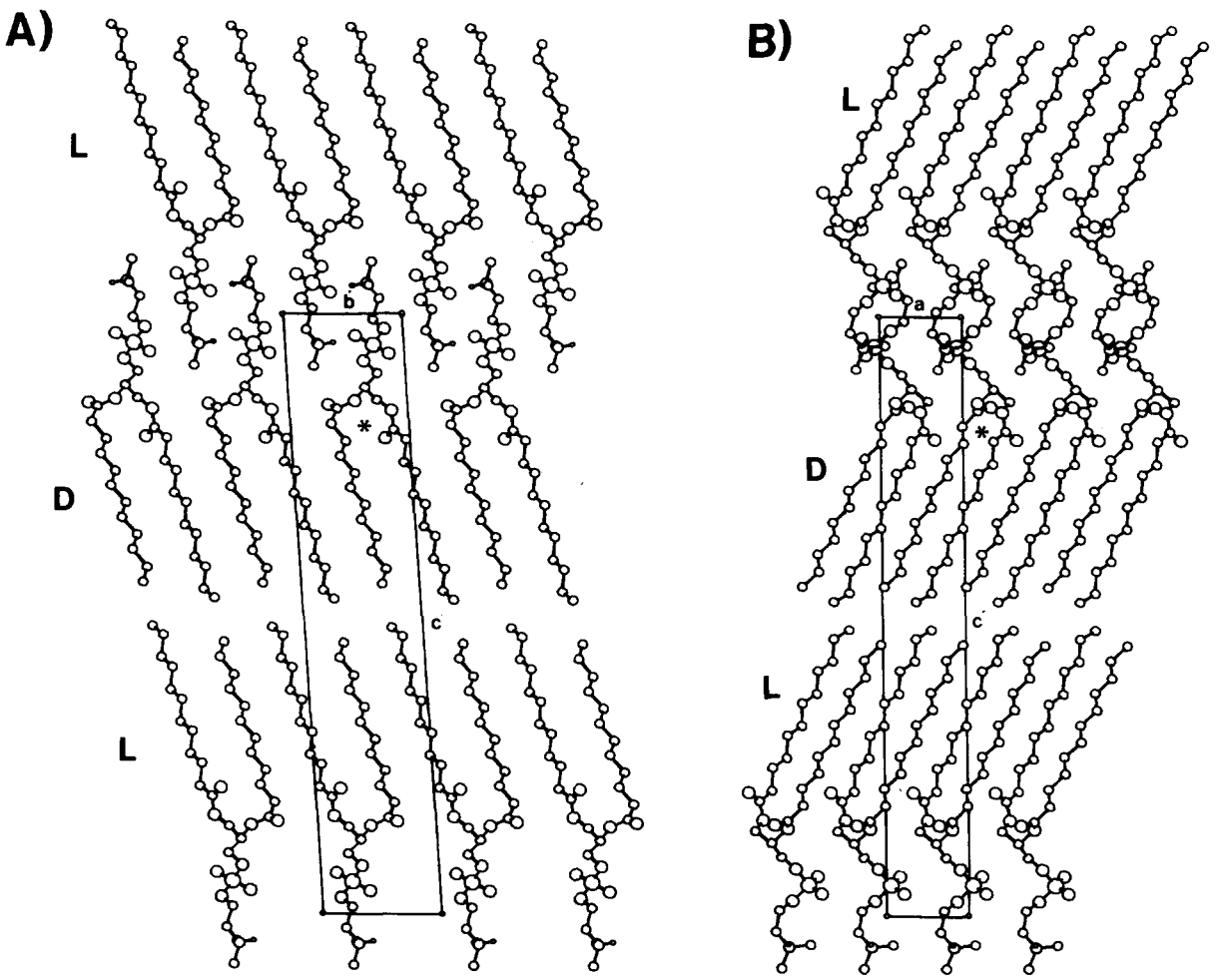

Fig. 2. Molecular packing of $DLPEM_2$ in views (A) along the *a* axis and (B) along the *b* axis. Note that molecules with D and L configuration pack in separate layers. For the molecule marked with an asterisk the coordinates are given in Table I.

places the two oxygens (O(21) and O(31) in a $-sc$ position to each other ($\theta_4 = -60°$) on one side of the glycerol plane.

The two hydrocarbon chains extend almost perpendicular (107°) to the glycerol plane. The γ-chain has a straight planar conformation. At the ester link there is a minor twist about the C(3)–O(31) bond ($\gamma_1 = 129°$) which give the chain a tilt of 33° with respect to the layer normal. The β-chain bends off by 60° at carbon atom C(22) due to a $-sc$ twist ($\beta_3 = -57°$) about the C(22)–C(23) bond and thus aligns parallel to the γ-chain.

The phosphodimethylethanolamine chain shows the well-known preferred conformational features observed for zwitterionic phosphocholine and phosphoethanolamine groups [9,17,18]. The torsion angle sequence $\alpha_1 = ap$, $\alpha_2/\alpha_3 = +sc/+sc$ $\alpha_4 = ac$ and $\alpha_5 = -sc$ are practically identical with that of, for example, dimyristoylphosphatidylcholine [19] (see Table II).

Discussion

The structure of $DLPEM_2$ reveals a number of new, interesting features regarding: (i) orientation and packing of the head groups; (ii) interaction of the dimethylamino group and; (iii) conformation of the diacylglycerol part. These structural proper-

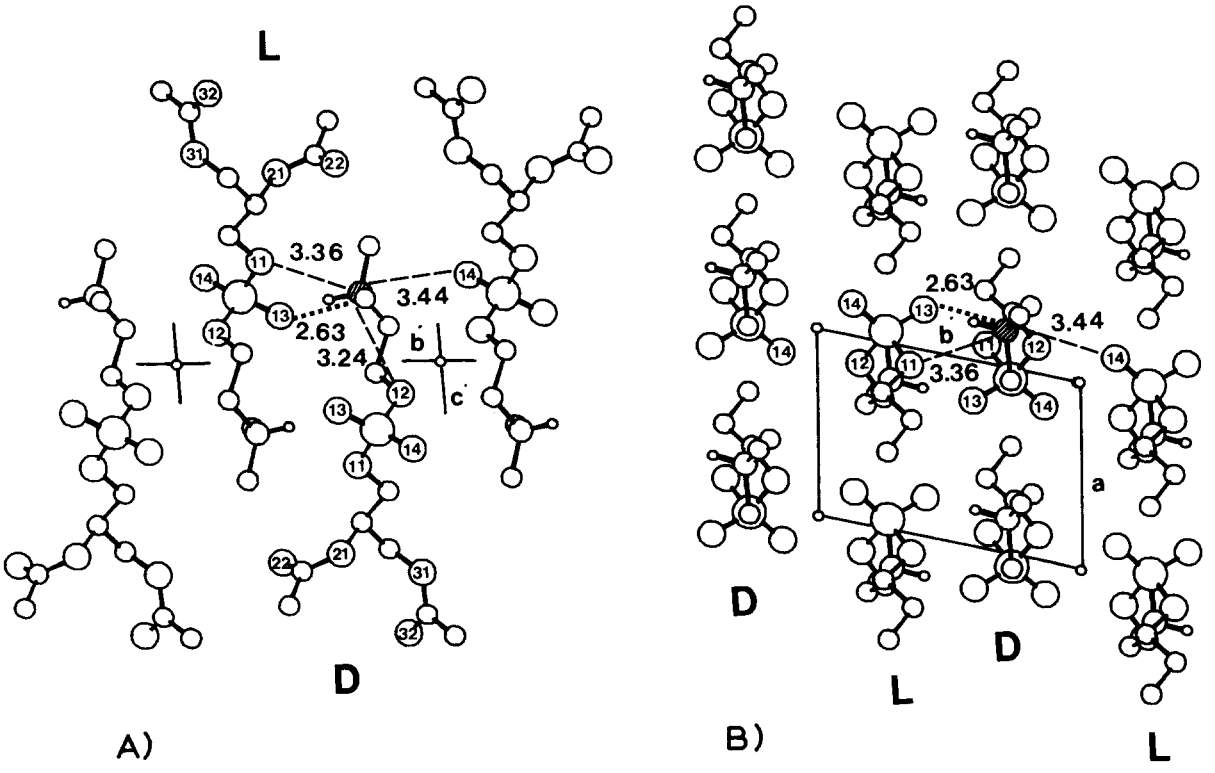

Fig. 3. Polar group arrangement and interactions in views (A) parallel and (B) perpendicular to the bilayer interface. The N–H hydrogen bond is indicated by dotted lines, electrostatic contacts by broken lines. The inter- and intramolecular contact distances given in Å. Note that in (B) one of the *N*-methyl groups obscures the C(11)–N(1) bond.

ties will now be discussed in relation to those of related glycerophospholipids.

Head group orientation

Usually zwitterionic head groups of phosphocholine or phosphoethanolamine lipids adopt an orientation parallel to the bilayer surface [9,18]. This dipole orientation with (+) and (−) charges aligned in one plane gives an electrostatically neutral head group layer without charge separation in the direction of the layer normal. This arrangement has been observed in a number of single-crystal structures [17,20,21] and has proved to be the most stable head group conformation in multi and single bilayer structures in contact with water [18,22].

The head group of $DLPEM_2$ deviates from this orientation. The *P–N* dipoles extend perpendicu-

TABLE II

TORSION ANGLES

For torsion angle notation see Ref. 9. DMPC, dimyristoylphosphatidylcholine [9,19]; DLPA, dilauroylphosphatidic acid monohydrate (Pascher and Sundell, unpublished data).

	α_1	α_2	α_3	α_4	α_5	θ_1	θ_2	θ_3	θ_4	β_1	β_2	β_3	β_4	γ_1	γ_2	γ_3	γ_4
$DLPEM_2$	179	65	54	144	−96	176	−66	56	−60	148	173	−57	176	129	−167	166	175
DMPC (1)	163	62	68	143	−64	58	177	−178	63	82	172	−81	45	−177	168	−173	178
DLPA	−151					64	−171	−172	62	83	174	164	173	−173	−176	−77	70

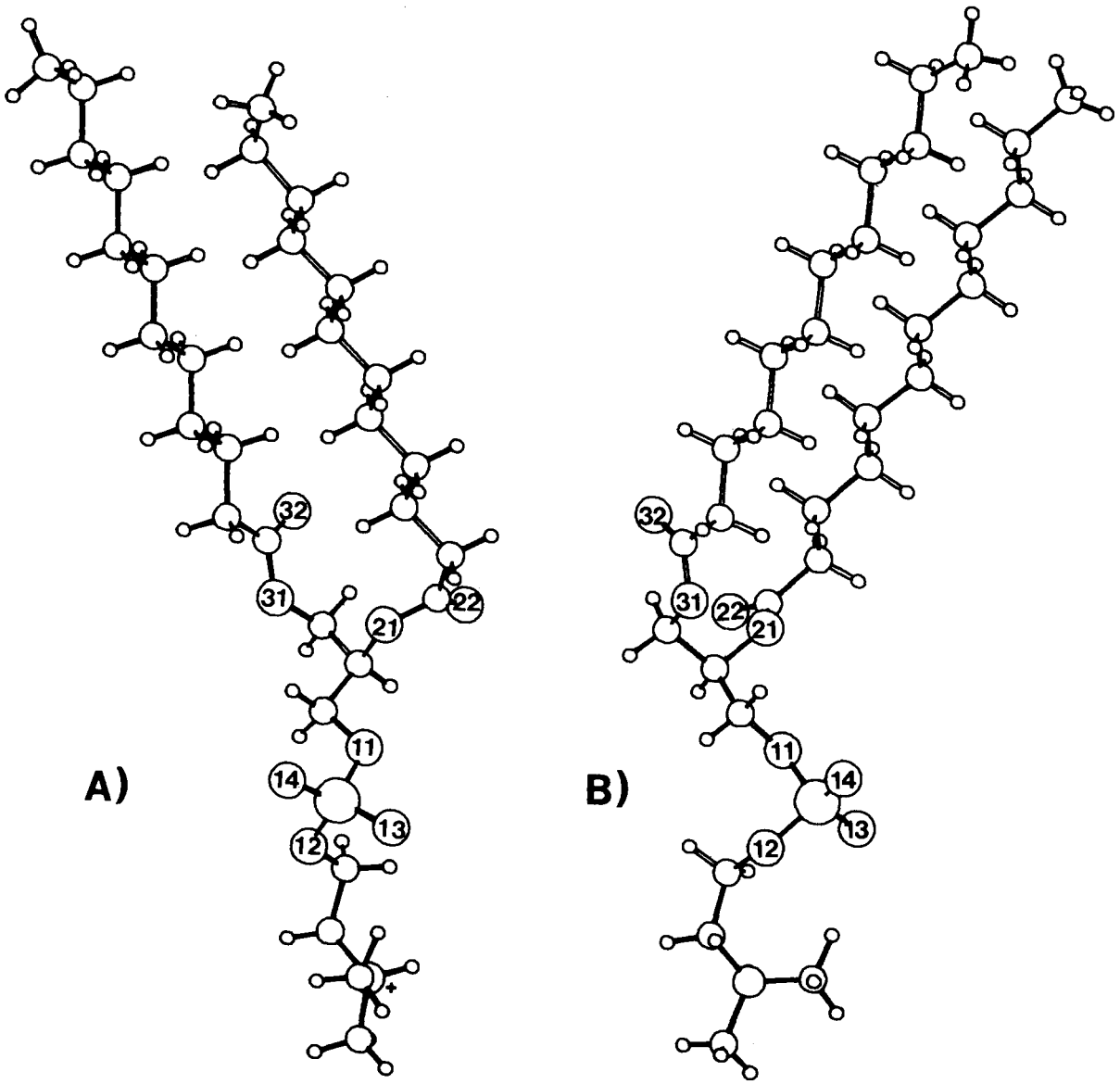

Fig. 4. Molecular conformation of $DLPEM_2$ (natural D enantiomer) in views (A) along the *a* axis and (B) along the *b* axis.

lar rather than parallel to the layer plane. From an electrostatic point of view this head group orientation is possible only in structures with stacked bilayers where the *P–N* dipoles of adjacent bilayers can interdigitate and thus preserve electroneutrality.

With respect to charge distribution and packing cross-section ($S = 45$ Å^2) this arrangement with layer-perpendicular interdigitating dipoles appears to be practically equivalent to that of layer-parallel dipoles arranged in two separate planes at both sides of the bilayer interface.

The reason why $DLPEM_2$ adopts the interdigitating head group arrangement is not quite obvious, but it might be favoured by specific polar interactions (see below). A transition of the head group dipoles from a layer-perpendicular to a layer-parallel orientation would be easily achieved

either by rotating the head group about the C(1)–C(2) glycerol bond or by an inversion of all α-torsion angles of the head group chain. Fig. 5A and B shows the rotation of the head-group about C(1)–C(2) by $\pm 120°$, into the two other staggered low-energy positions (θ_1 from *ap* to $+sc$ and $-sc$). Fig. 5C shows the change in head group orientation resulting from an inversion of the torsion angles α_1–α_5 (bond C(1)–O(11) to C(11)–C(12)). In all these head group reorientations (Fig. 5A–C) the typical preferred conformation of the zwitterionic phosphoethanolamine group [9,17] is preserved. In the case of α-chain inversion (Fig. 5C) the headgroup changes between energetically identical image–mirror image conformations. The conformational changes demonstrated in Fig. 5 should not significantly affect the overall charge distribution and packing cross-section of the phosphodimethylethanolamine head groups at the bilayer-bilayer interface.

The distance between the two planes comprising the (+) and (−) charges in $DLPEM_2$ is 4.0 Å. The corresponding distances of the separate phosphocholine dipole layers in lauroyl-2-deoxy-PC [21] and phosphoethanolamine dipole layers in palmitoyl-lyso-PE [17] are 4.3 and 3.4 Å, respectively, compatible with that of $DLPEM_2$. The minor differences in the interlayer distance reflect changes in intermolecular bonding distances due to the *N*-methyl groups.

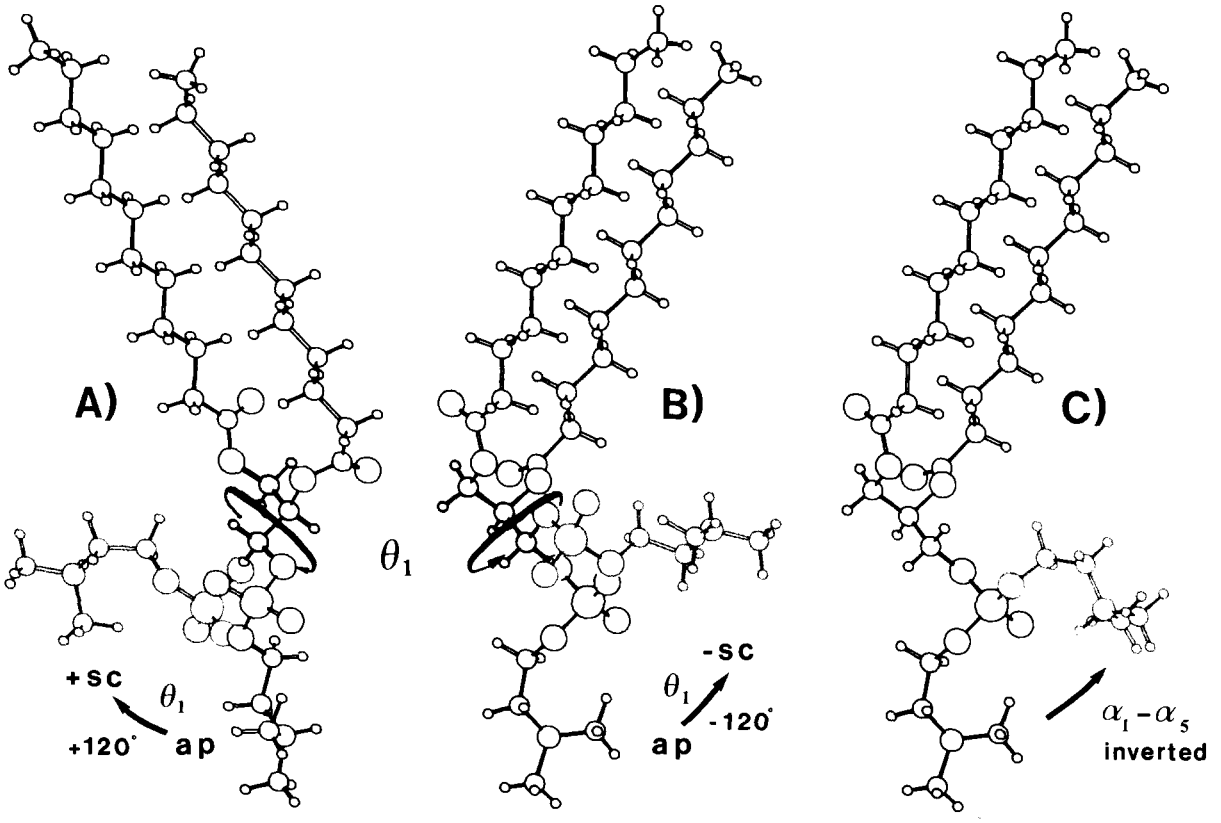

Fig. 5. Reorientation of the head group dipole in $DLPEM_2$ form layer-perpendicular to layer-parallel. (A) Rotation (+120°) of the head group about the C(1)–C(2) glycerol bond; θ_1 from *ap* to $+sc$. (B) Rotation (−120°) of the head group about the C(1)–C(2) glycerol bond; θ_1 from *ap* to $-sc$. (C) Inversion of the torsion angles $\alpha_1-\alpha_5$ of the head group chain (bond C(1)–O(11) to C(11)–C(12)) to mirror image conformation. In all three models the typical minimum-energy conformation of the zwitterionic phosphoethanolamine chain is preserved. In order to show clearly the change in head group orientation different projections (molecule A along the *a* axis and B and C along the *b* axis) were chosen.

Specific head group interactions

The unsubstituted and the fully methylated ethanolamine groups show very different interaction principles. The unmethylated ammonium group, e.g. in dilauroyl-PE [20] or palmitoyl-lyso-PE [17], interacts by short intermolecular bonds (2.6–2.7 Å) with unsubstituted oxygens of the phosphate group. These bonds have the character of hydrogen bonds, superimposed by an ionic bond. The contacts are directed along the tetrahedral axis of the ammonium nitrogen in extension of the N–H... bonds. These strong interactions give rise to a rigid, tightly bound packing pattern of the phosphoethanolamine group with a cross-sectional area of 36–40 $Å^2$.

The quaternary choline group, on the other hand, establishes rather long electrostatic bonding contacts (3.7–4.3 Å) towards phosphate oxygens. The choline group thereby also favours the formation of intermolecular bonds along the tetrahedral axes of the nitrogen atom. But, differing from $-NH_3^+$, the (−) ligands approach the nitrogen in the reverse direction, along the $...N–CH_3$ axes to establish the closest contact to the (+) charge. Furthermore, the phosphate groups bind a water molecule (or other proton donator) which links the phosphate group into rows. In these arrangements the phosphocholine monohydrate requires a packing cross-section of 50–52 $Å^2$ [9].

For phosphoethanolamine lipids with partially methylated nitrogen atoms, such as $DLPEM_2$, both of the interaction principles described for the ammonium group apply. This leads to specific interaction conditions, as bond contacts form both in extension of the N–H... and the ...N–C(H) axes.

As shown in Fig. 3A and B, the ammonium nitrogen interacts with two bonds towards one of the adjacent phosphate groups. This becomes possible because the axis of the N–H... hydrogen bond intersects with the axes of three possible electrostatic contacts at a small angle of 70°. This greatly favours a selective interaction of the $-NH(CH_3)_2$ group with two oxygens of one single phosphate group, rather than a more uniform interaction with oxygens of three neighbouring phosphate groups.

Conformation of the diacylglycerol group

Crystal structure analyses and NMR studies show that in glycerophospholipids the diacylglycerol moiety adopts a specific preferred conformation which predominates both in the solid [9,23], the gel and the liquid crystalline state [18,24] and also in micelles and the monomeric form (Ref. 25 and unpublished data). The characteristic basic feature of this diacylglycerol structure is an *ap* conformation about the glycerol C(2)–C(3) bond, which arranges the four atoms C(1)–C(2)–C(3)–O(31) of the glycerol backbone in a planar chain. In a bilayer structure this glycerol backbone is oriented either perpendicular or parallel to the bilayer plane (compare Fig. 6B and C).

In the 'perpendicular' position the glycerol backbone together with the γ-chain forms a planar zigzag chain extending in the direction of the layer normal. From this straight chain the β-fatty acid branches off layer-parallel, but makes a 90° bend, in order to stack parallel to the γ-chain (Fig. 6B).

In structures with the glycerol backbone in the 'layer-parallel' position the β-chain extends straight in the direction of the layer normal and the γ-chain bends off by 90° (Fig. 6C).

In crystal structures the layer-perpendicular glycerol chain orientation (Fig. 6B) has been observed in dilauroyl-PE [20] and dimyristoyl-PC [19]. (A similar orientation has also been shown for the corresponding ceramide part in cerebroside [23,26].) The layer-parallel glycerol orientation (Fig. 6C) has been found in the crystal structure of dilauroylglycerol [23], dimyristoyl-PA [27] and dilauroyl-PA monohydrate (Pascher and Sundell, unpublished data).

In $DLPEM_2$ the glycerol backbone has a $+sc$ instead of an *ap* conformation about the C(2)–C(3) bond. Compared to the structure in Fig. 6B this difference is produced by an anti-clockwise 120° rotation of the entire γ-chain about the C(2)–C(3) glycerol bond, (θ_3: $ap \rightarrow +sc$). The two fatty acid-substituted glycerol oxygens O(21) and O(31) thereby change their mutual position θ_4 from $+sc$ to $-sc$.

As the hydrocarbon chains are constrained to maintain an approximately layer-perpendicular extension in the chain matrix, the rotation about C(2)–C(3) causes the glycerol chain to turn from a layer-perpendicular to a 45°-inclined orientation.

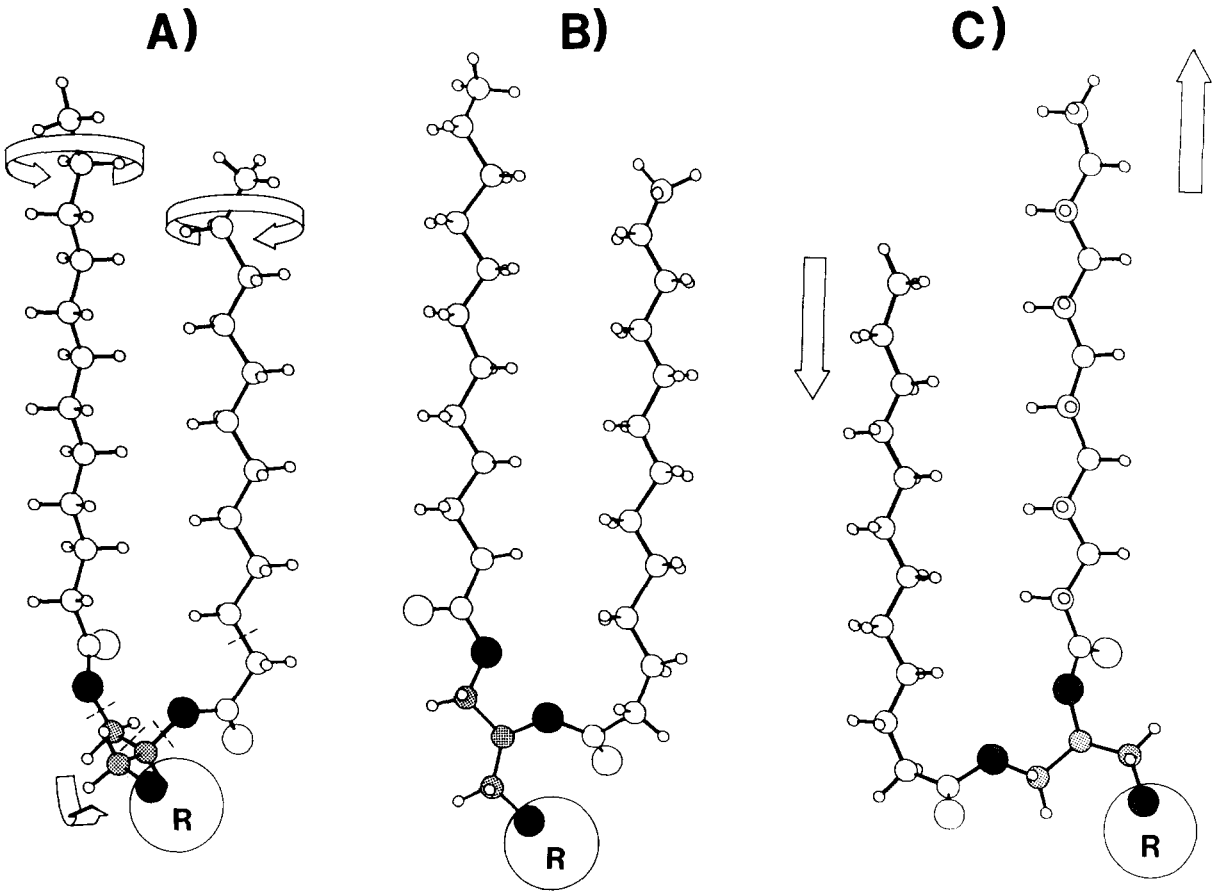

Fig. 6. Preferred conformations of the diacylglycerol moiety as observed in (A) $DLPEM_2$, (B) dimyristoyl-PC [19] and (C) dilauroyl-PA monohydrate (Pascher and Sundell, unpublished data). The arrows indicate the motion of the hydrocarbon chains causing the transitions of B to A and C, respectively.

Concurrently the β-chain rotates 120° clockwise about the C(22)–C(23) bond (β_4: *sc* → *ap*) in order to restore a parallel chain stacking. This conformation has also been observed in the crystal structure of 2,3-di(11-bromo-undecanoyl)-DL-glycero-*p*-toluensulfonate [28], as well as in $DLPEM_2$.

The differences between the three conformations of the diacylglycerol part shown in Fig. 6 thus arise from rotational motions and axial translations of the hydrocarbon chains.

The transition of conformation B to A comes about by a 120° clockwise/anti-clockwise rotation of the β- and γ-chains which changes the orientation of the glycerol chain from a layer-perpendicular to a 45°-inclined position.

The transition from conformation B to C proceeds by an axial displacement of the two hydrocarbon chains by 4 methylene units. The glycerol backbone thereby turns from a layer-perpendicular to a layer-parallel position. The β-chain straightens out and the γ-chain becomes bent.

NMR studies have shown that in aqueous dispersion and monomeric solution of ethanolamine and choline phospholipids the conformers shown in Fig. 6A and B coexist with a fractional population of about 30 and 60%, respectively (Ref. 25 and unpublished data). The existence of the conformer with a layer-parallel glycerol group (Fig. 6C) has so far not been confirmed in systems other than the solid state. At present NMR analyses of phospholipids with a selectively deuterated glycerol group are performed to study the population and

transitions of the three conformers in lipid-water systems.

Acknowledgements

We are grateful to Max Lundmark for skillful technical assistance. The work is supported by the Swedish Medical Research Council (grant 006) and the Alice and Knut Wallenberg foundation.

References

1 Bremer, J. and Greenberg, D.M. (1962) Biochim. Biophys. Acta 45, 205–216
2 Kates, M. and Wassef, K.M. (1970) Biochemistry 39, 323
3 Hirata, F. and Axelrod, J. (1978) Nature (London) 275, 219–220
4 Hirata, F. and Axelrod, J. (1980) Science 209, 1082–1090
5 Fain, J.N. (1982) in Hormone Receptors, Horizons in Biochemistry and Biophysics (Korn L.D., ed.), Vol. 6, pp. 237–276, John Wiley and Sons, New York
6 Casal, H.L. and Mantsch, H.H. (1983) Biochim. Biophys. Acta 735, 387–396
7 Mulukutla, S. and Shipley, G.G. (1984) Biochemistry 23, 2514–2519
8 Quinn, P.J. (1980) Prog. Biophys. Mol. Biol. 38, 1–104
9 Hauser, H., Pascher, I., Pearson, R. and Sundell, S. (1981) Biochim. Biophys. Acta 650, 21–51
10 Main, P., Hull, S.E., Lessinger, L., Germain, G., Declercq, J.P. and Woolfson, M.M. (1978) MULTAN 78. A System of Computer Programs for the Automatic Solution of Crystal Structures from X-ray Diffraction Data. Universities of York, England, and Louvain, Belgium
11 Beurskens, P.T., Bosman, W.P.J.H., Doesburg, H.M., Gould, R.O., Van den Hark, T.E.M., Prick, P.A.J., Noordik, J.H., Beurskens, G. and Parthasarathi, V. (1981) Technical Report 1981/2, Crystallography Laboratory, Toernooiveld, 6525 ED Nijmegen, The Netherlands
12 Mills, O.S. and Rollet, J.S. (1961) Computing Methods and the Phase Problem in X-ray Crystal Analysis, pp. 107–124, Pergamon, London
13 Cromer, D.T. and Mann, J.B. (1968) Acta Crystallogr. A24, 321–324
14 Stewart, J.M., Kruger, G.J., Ammon, H.L., Dickinson, C. and Hall, S.R. (1972) The X-ray System – version of June 1972. Technical Report TR-192, Computer Science Center, University of Maryland, College Park
15 Sundaralingam, M. (1972) Ann. N.Y. Acad. Sci. 195, 324–355
16 Abrahamsson, S., Dahlen, B., Löfgren, H. and Pascher, I. (1978) Prog. Chem. Fats Lipids, 16, 125–143
17 Pascher, I., Sundell, S. and Hauser, H. (1981) J. Mol. Biol. 153, 807–824
18 Seelig, J. and Seelig, A. (1980) Q. Rev. Biophys. 13, 19–61
19 Pearson, R. and Pascher, I. (1979) Nature (London) 281, 499–501
20 Elder, M., Hitchcock, P.B., Mason, R. and Shipley, G.G. (1977) Proc. R. Soc. Ser. A, 354, 157–170
21 Hauser, H., Pascher, I. and Sundell, S. (1980) J. Mol. Biol. 137, 249–264
22 Seelig, J. (1978) Biochim. Biophys. Acta 515, 105–140
23 Pascher, I., Sundell, S. and Hauser, H. (1981) J. Mol. Biol. 153, 791–806
24 Davis, J.H. (1983) Biochim. Biophys. Acta 737, 117–171
25 Hauser, H., Guyer, W., Pascher, I., Skrabal, P. and Sundell, S. (1980) Biochemistry 19, 366–373
26 Pascher, I. and Sundell, S. (1977) Chem. Phys. Lipids 20, 175–191
27 Harlos, K., Eibl, H., Pascher, I. and Sundell, S. (1984) Chem. Phys. Lipids 34, 115–126
28 Watts, P.H., Jr., Pangborn, W.A. and Hybl, A. (1972) Science 175, 60–61